Am J Cancer Res 2024;14(6):2839-2851
www.ajcr.us /ISSN:2156-6976/ajcr0153561

Original Article

SLC11A1 predicts the overall survival of patients with colorectal cancer

Hung-Chih Hsu[1,2], Yun-Shien Lee[3,4], Titilianty I Imbang[5], Ting-Chia Liu[6], Shuen-Iu Hung[5,6]

[1]Division of Hematology-Oncology, Chang Gung Memorial Hospital, Linkou Branch, Taoyuan 333, Taiwan; [2]College of Medicine, Chang Gung University, Linkou, Taoyuan 333, Taiwan; [3]Genomic Medicine Research Core Laboratory, Chang Gung Memorial Hospital, Linkou Branch, Taoyuan 333, Taiwan; [4]Department of Biotechnology, Ming-Chuan University, Taoyuan 333, Taiwan; [5]Cancer Vaccine and Immune Cell Therapy Core Lab, Chang Gung Immunology Consortium, Department of Medical Research, Chang Gung Memorial Hospital, Linkou Branch, Taoyuan 333, Taiwan; [6]Institute of Pharmacology, School of Medicine, National Yang Ming Chiao Tung University, Taipei 112, Taiwan

Received September 22, 2023; Accepted April 21, 2024; Epub June 15, 2024; Published June 30, 2024

Abstract: Colorectal cancer (CRC) remains a significant contributor to cancer-related mortality, emphasizing the critical need for identifying biomarkers that can improve clinical management and patient outcomes. In this retrospective study, we analyzed tumor samples from 25 patients with metastatic CRC, categorized based on long-term (> 50 months) or short-term (< 10 months) survival. Employing the PanCancer Immune Profile Panel, encompassing 770 genes, in the discovery dataset, we identified 54 differentially expressed genes (DEGs) within the tumor microenvironment of metastatic CRC. Validation of potential biomarkers was performed using two publicly available RNA-based sequencing datasets (TCGA 1 (n=371) and TCGA 2 (n=566)). Univariate COX regression unveiled that three significant biomarkers were associated with overall survival in CRC within the discovery dataset, which were SLC11A1 (hazard ratio (HR): 4.09, P=0.012), TNFSF11 (HR: 3.67, P=0.02), and MEF2C (HR: 0.34, P=0.037). Kaplan-Meier survival curve analyses confirmed the correlation between SLC11A1 expression and overall survival in CRC across the discovery set (P=0.0071) and the two independent datasets (TCGA 1 (P=0.0016) and TCGA 2 (P=0.025)). Receiver operating characteristic curve analysis demonstrated an area under the curve ranging from 0.64 to 0.76, with sensitivity of 59% to 87% and specificity of 60% to 73% for predicting CRC overall survival. Immunohistochemistry staining further validated the strong expression of SLC11A1 protein in CRC tumor cells, with high expression correlating with short-term survival. These findings suggest that SLC11A1 serves as a predictive biomarker for overall survival in CRC patients.

Keywords: Colorectal cancer, SLC11A1, prognostic marker, biomarker, overall survival

Introduction

Colorectal cancer (CRC) is one of the most aggressive malignancies, contributing to approximately two million new cases and one million deaths in 2020 [1]. The incidence of CRC is the third-highest cancer worldwide and is the second leading cause of cancer-related mortality [1]. According to data from the American Cancer Society, the overall 5-year survival rate for CRC at all stages is around 65%; the survival rate, however, plummets to about 13% for patients in the metastatic phase [2-4]. Despite the combination of different cytotoxic chemotherapies, targeted therapeutic interventions, and radiotherapy for the treatment, the disease prognosis and patient outcomes of CRC still need improvement [5]. Identifying biomarkers for CRC could revolutionize clinical management, enhance patient survival, and catalyze the development of novel therapeutic strategies [6, 7].

Recent evidence suggests that immune mediators in the tumor microenvironment (TME) play an essential role in the disease prognosis and impact the clinical outcomes of CRC [8-10]. The TME comprises a complex milieu encompassing the extracellular matrix and various cellular components, including cancer cells, stromal

https://doi.org/10.62347/VTYU3157

cells, fibroblasts, adipocytes, and tumor-infiltrating immunocytes, such as tumor-associated macrophages, dendritic cells, myeloid-derived suppressor cells, natural killer cells, and tumor-infiltrating lymphocytes [11]. Cancer cells interact with the immunocytes expressing various receptors, transporters, cytokines, chemokines, and cytotoxic proteins, and all collectively determine the dynamic landscape of the cancer-immunity microenvironment [12]. Elements within the TME hold significant promise as therapeutic targets, exerting profound impacts on disease prognosis [13-16].

To investigate biomarkers associated with the overall survival of CRC, we retrospectively collected RNA samples from (FFPE) tumor tissues of 25 patients with metastatic CRC (15 with long-term survival for more than 50 months, and 10 with short-term survival less than 13 months) in this study. We analyzed the transcriptome of TME by the PanCancer Immune Profile Panel with 770 genes, and the differentially expressed genes (DEGs) by volcano plots, pathway analysis, univariate COX regression, and Kaplan-Meier overall survival curves. We further validated the data by two independent datasets (TCGA 1 (n=371) and TCGA 2 (n=566)), which were RNA-based sequencing. We estimated the predictive performance of the biomarker by receiver operating characteristic (ROC) curve analysis. The expression of identified biomarker was validated by immunohistochemistry.

Materials and methods

Sample collection for the discovery dataset

To establish the discovery dataset, we retrospectively obtained the formalin-fixed paraffin-embedded (FFPE) tumor tissue of 25 patients with metastatic CRC. The clinical information, including demographic information, clinical characteristics, histopathological features, *KRAS* mutation status, and response to targeted therapies, was collected from the medical records. The response to the targeted therapy was evaluated by imaging according to the Response Evaluation Criteria in Solid Tumors (RECIST). This study was reviewed and approved by the Ethics Committee of the Institutional Review Board of Chang Gung Memorial Hospital and complied with the Declaration of Helsinki. Each participant provided written informed consent.

Validation datasets

We used two independent datasets from The Cancer Genome Atlas (TCGA) of cBioPortal to validate the biomarkers identified from the discovery dataset. The first dataset, TCGA 1, was obtained from Colorectal Adenocarcinoma (TCGA, Firehose Legacy), which consists of RNA Seq (V2 RSEM) data of the CRC tumor samples of 371 patients (https://www.cbioportal.org/study/summary?id=coadread_tcga). The second dataset, TCGA 2, was obtained from PanCancer Atlas, which includes RNA Seq (V2 RSEM) data of the CRC tumor samples of 566 patients (https://www.cbioportal.org/study/summary?id=coadread_tcga_pan_can_atlas_2018) [17].

Gene expression analysis, visualization, and pathway analysis

The FFPE sections were macro-dissected from the blocks for RNA extraction by the AllPrep RNA FFPE Kit (Qiagen, Venlo, Netherlands). The samples were quantified using the NanoDrop (ND1000, TermoFisher Scientific, Waltham, MA, USA), and qualified by a Qubit 3.0 RNA Hi-Sensitivity analysis kit (Life Technologies, Carlsbad, CA, USA), and the NanoString workflow.

The transcriptome of RNA samples was analyzed by NanoString nCounter PanCancer Immune Profile Panel (NanoString Technologies, Seattle, WA, USA). The digital barcodes representing the number of transcripts of the sample were counted by NanoString nCounter Digital Analyzer (NanoString Technologies). To eliminate the variability between samples, we normalized the raw data using nSolver Analysis software based on the normalization factor by the geometric mean of the housekeeping genes of samples. Normalized data were $\log_2$ (Fold Change of expression)-transformed for analyses [18]. The R package and clusterProfiler were used to annotate DEGs, and the data was examined by Gene Ontology functional enrichment analysis for GO-BP (Gene Ontology biological pathway) [19, 20]. The difference in DEG expression with adjusted *P*-value < 0.05 was considered significant. The potentially involved

pathways were examined by cross-referencing the pathway score.

Analysis of the association between biomarkers and the survival probability

We performed univariate COX regression hazard ratio analyses and multivariate logistic regression to examine the association between DEGs and the overall survival of CRC. Kaplan-Meier curve analysis was performed to estimate the distributions of patient survival, and the statistical significance of apparent differences in survival between groups was tested using the log-rank test. P value < 0.05 was considered significant.

Receiver operating characteristic curve and area under the curve analyses

We constructed the ROC curve and area under the curve (AUC) to evaluate the sensitivity and specificity of the DEG for survival prediction. The median gene expression level was used as the cut-off value. The AUC, P value, and confidence interval were calculated using the MedCalc software version 19.2.1.

Immunohistochemistry analysis

The formalin-fixed, paraffin-embedded tissues were sectioned at a thickness of 3-5 μm (Leica rm2125 RTS, Leica, US). Paraffin section slides underwent deparaffinization and rehydration. To expose target proteins, antigen retrieval was performed using 10 mM sodium citrate (pH 6.0), which was heated by microwave oven for 8 to 15 minutes. Following antigen retrieval, endogenous peroxidase activity was blocked in 3% hydrogen peroxide solution for 15 minutes at room temperature. The slides were then incubated overnight at 4°C with rabbit anti-human SLC11A1 antibody (Abcam, ab211448, USA). After three times of PBS buffer washing, the slides were treated with secondary antibodies (goat anti-rabbit IgG), followed by additional washing steps and incubation with rabbit peroxidase-anti-peroxidase (Jackson ImmunoResearch, PA, USA). The reactivity was visualized using a DAB (3,3'-diaminobenzidine) substrate chromogen solution. Finally, slides were counterstained with hematoxylin, dehydrated, and mounted.

Statistical analysis

We performed Fisher's exact test, Chi-square test, unpaired (2-tailed) Student's t-test, univariate COX regression analysis, and multivariate logistic regression analysis using PASW Statistics 18 (SPSS, Chicago, Illinois, USA). The data are reported as means, standard error of the mean (SEM), standard deviation (SD), ranges, or percentages. A value of $P \leq 0.05$ was considered significant.

Results

Clinical characteristics of enrolled metastatic CRC patients

A total of 25 metastatic CRC patients were included in the discovery study and categorized into two distinct groups: short-term survivors (n=10) with an overall survival of less than 13 months and long-term survivors (n=15) who exhibited an overall survival exceeding 50 months (**Table 1**). A significant difference was noted in age at the time of diagnosis between the two groups (P=0.043). Notably, long-term survivors displayed a mean age of 53.13 years, while short-term survivors had an average age of 63.10 years (**Table 1**). Conversely, sex distribution exhibited no variations.

The overall survival significantly differs between the two groups (P < 0.0001). Short-term survivors displayed a median overall survival of 10.5 months, markedly lower than the median overall survival of 59.3 months observed in long-term survivors (**Table 1**). Histological data demonstrated differences between the two groups (P=0.0005); however, no differences in the frequencies of synchronous versus metachronous tumors were observed (**Table 1**). In addition, a significant variation in tumor sidedness was noted (P=0.03), with 93.3% of long-term survivors presenting with left-sided tumors, while only 50% of short-term survivors exhibited similar tumor localization (**Table 1**). No significant differences were identified in *KRAS* mutation status, but responses to anti-EGFR and anti-VEGF targeted therapies were significantly elevated in long-term survivors (P=0.007 and P=0.048, respectively) (**Table 1**).

Differential expression of genes in the metastatic CRC tumor microenvironment

We conducted a comprehensive analysis of the expression profiles of 770 human immune-related genes within the TME of metastatic CRC patients using the PanCancer Immune Profile Panel multiplex gene expression assay by Nanostring Technologies. The resulting volcano

Table 1. Clinicopathological features of the enrolled metastatic CRC patients

Clinical characteristics	Short-term survivors (OS < 13 months)	Long-term survivors (OS > 50 months)	*P*-value*
Age (year)			
Mean ± SD (range)	63.10 ± 3.3 (48~73)	53.13 ± 3.1 (34~76)	0.043
Sex, n (%)			
Male	6 (60.0%)	7 (46.7%)	
Female	4 (40.0%)	8 (53.3%)	0.52
Overall survival (OS) (month)			
Median (range)	10.5 (4.5~12.7)	59.3 (50~84)	< 0.0001
Histology, n (%)			
Well differentiation	2 (20%)	2 (13.3%)	
Moderate differentiation	6 (60%)	13 (86.7%)	
Poor differentiation	2 (20%)	0 (0%)	0.0005
Synchronous/Metachronous, n (%)			
Synchronous	7 (70%)	10 (66.7%)	
Metachronous	3 (30%)	5 (33.3%)	0.86
Tumor sidedness, n (%)			
Left-side	5 (50%)	14 (93.3%)	
Right-side	5 (50%)	1 (6.7%)	0.030
KRAS gene mutations, n (%)			
Mutant	3 (30%)	1 (6.7%)	
Wild-type	7 (70%)	14 (93.3%)	0.27
Response to Targeted therapy, n (%)			
Anti-EGFR			
Responders (PR CR)	0 (0%)	6 (75%)	
Non-responders (SD PD)	7 (100%)	2 (25%)	0.007
Anti-VEGF			
Responders	0 (0%)	5 (83.3%)	
Non-responders	3 (100%)	1 (16.7%)	0.048

*The differences in age and overall survival between the two groups were compared by two-tailed independent t-tests, and the other characteristics were analyzed by two-tailed Fisher's exact tests.

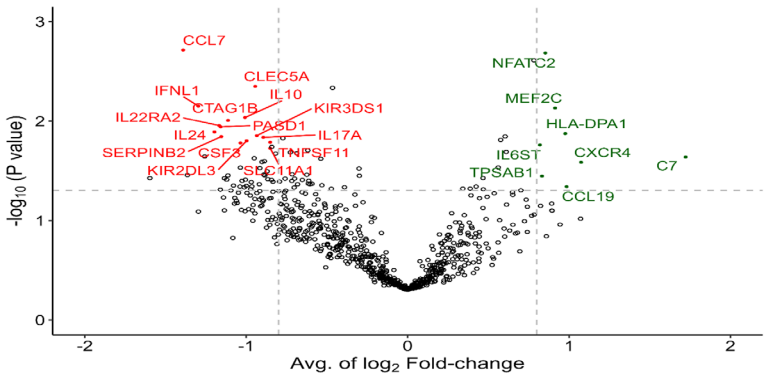

Figure 1. Identification of 54 differentially expressed genes (DEGs) in TME associated with overall survival of metastatic CRC using the discovery dataset. The volcano plot illustrates DEGs obtained from a comparison of gene expression between long-term survivors and short-term survivors. The y-axis represents the -$\log_{10}$ of the adjusted *P*-value, while the x-axis displays the $\log_2$ fold-change in gene expression. Thresholds are indicated by gray lines set at adjusted $P < 0.05$ and $|\log_2$ fold-change$| > 0.8$. Red circles represent DEGs with significantly increased expression in short-term survivors, while green circles represent DEGs with significantly increased expression in long-term survivors.

plot unveiled 54 DEGs exhibiting significant differences in their expression levels within the TME when comparing the two patient groups (**Figure 1**). Among these DEGs, eight were found to be up-regulated, while 46 were down-regulated in the TME of long-term survivors in comparison to their short-term counterparts (**Table 2**).

To gain insights into the biological pathways associated with the up-regulated DEGs within the TME of long-term survivors, we performed Gene Ontology (GO) enrichment analysis. This analysis highlighted that the DEGs, including

Table 2. Differentially expressed genes (DEGs) with significant level changes within the tumor microenvironment of metastatic CRC in the discovery dataset

No.	DEGs*	*P*-value	Avg. Log_2FC
U1	NFATC2	2.07E-03	0.85
U2	MEF2C	7.38E-03	0.91
U3	HLA-DPA1	1.34E-02	0.98
U4	IL6ST	1.73E-02	0.82
U5	C7	2.30E-02	1.72
U6	CXCR4	2.60E-02	1.07
U7	TPSAB1	3.57E-02	0.83
U8	CCL19	4.55E-02	0.98
D1	CCL7	1.92E-03	-1.39
D2	CLEC5A	4.47E-03	-0.94
D3	IFNL1	7.05E-03	-1.30
D4	IL10	9.18E-03	-1.01
D5	CTAG1B	9.82E-03	-1.11
D6	IL22RA2	1.11E-02	-1.17
D7	PASD1	1.14E-02	-1.16
D8	IL24	1.29E-02	-1.20
D9	KIR3DS1	1.40E-02	-0.93
D10	SERPINB2	1.43E-02	-1.15
D11	IL17A	1.46E-02	-0.89
D12	KIR2DL3	1.58E-02	-1.00
D13	TNFSF11	1.63E-02	-0.85
D14	CSF3	1.66E-02	-1.04
D15	ARG2	1.81E-02	-0.84
D16	SLC11A1	1.87E-02	-0.85
D17	SYT17	2.12E-02	-0.82
D18	S100A12	2.27E-02	-1.26
D19	IL17B	2.37E-02	-0.95
D20	KLRD1	2.53E-02	-0.89
D21	CD244	2.58E-02	-0.90
D22	GATA3	2.94E-02	-1.04
D23	IL19	2.97E-02	-0.92
D24	KIR2DL1	3.20E-02	-0.87
D25	CCL3	3.45E-02	-0.89
D26	GAGE1	3.48E-02	-1.36
D27	FOXJ1	3.52E-02	-0.89
D28	SPACA3	3.52E-02	-1.11
D29	BAGE	3.74E-02	-1.60
D30	CCR3	3.75E-02	-1.14
D31	HAMP	3.84E-02	-0.87
D32	PLA2G1B	3.88E-02	-1.12
D33	CCL26	3.88E-02	-1.01
D34	NCR1	3.90E-02	-0.84
D35	IFNA1	3.98E-02	-1.03
D36	CXCR1	4.07E-02	-0.83
D37	MBL2	4.10E-02	-0.97
D38	IL1A	4.31E-02	-0.92
D39	IL2	4.44E-02	-1.08
D40	DEFB1	4.47E-02	-1.00
D41	IL13	4.53E-02	-0.97
D42	MAGEA1	4.55E-02	-1.04
D43	IL25	4.63E-02	-1.01
D44	CCL25	4.82E-02	-0.97
D45	IL27	4.88E-02	-1.16
D46	C8A	4.98E-02	-1.10

*The DEGs were identified by comparing the fold-change (FC) of gene expression in the tumor microenvironment between the long-term survivors and short-term survivors in the discovery dataset.

NFATC2, MEF2C, IL6ST, HLA-DPA1 and CCL19, are up-regulated in the positive regulation of lymphocyte proliferation ($P=5.67\times10^{-7}$), contributing to the long-term survival of metastatic CRC (**Figure 2A**). In contrast, the most significance within the TME of short-term survivors is cytokine mediated signaling pathway ($P=1.83\times10^{-3}$), which involves DEGs CLEC5A, SLC11A1, IL10, IL17A, and IFNL1 (**Figure 2B**). These findings shed light on the distinct molecular signatures characterizing the TME in long-term and short-term survivors of metastatic CRC, offering potential insights into the underlying mechanisms influencing patient survival.

Association between SLC11A1, TNFSF11, and overall survival in metastatic CRC

Univariate COX regression hazard ratio analysis identified three DEGs significantly associated with the survival of metastatic CRC in the discovery dataset. These DEGs included SLC11A1 (Solute Carrier Family 11 Member 1) (P=0.012), TNFSF11 (P=0.02), and MEF2C (P=0.037) (**Table 3**). Kaplan-Meier survival curve analyses further supported the significant associations between these three DEGs and the survival of metastatic CRC (SLC11A1 (P=0.0071), TNFSF11 (P=0.013), and MEF2C (P=0.03)) (**Figure 3**).

Incorporating significant clinical variables (age, histology, and tumor sidedness) alongside the three DEGs (SLC11A1, TNFSF11, and MEF2C) in the univariate COX regression analysis revealed that both SLC11A1 (P=0.012) and TNFSF11 (P=0.02) retained their significance in predicting the overall survival of CRC (**Table 4**).

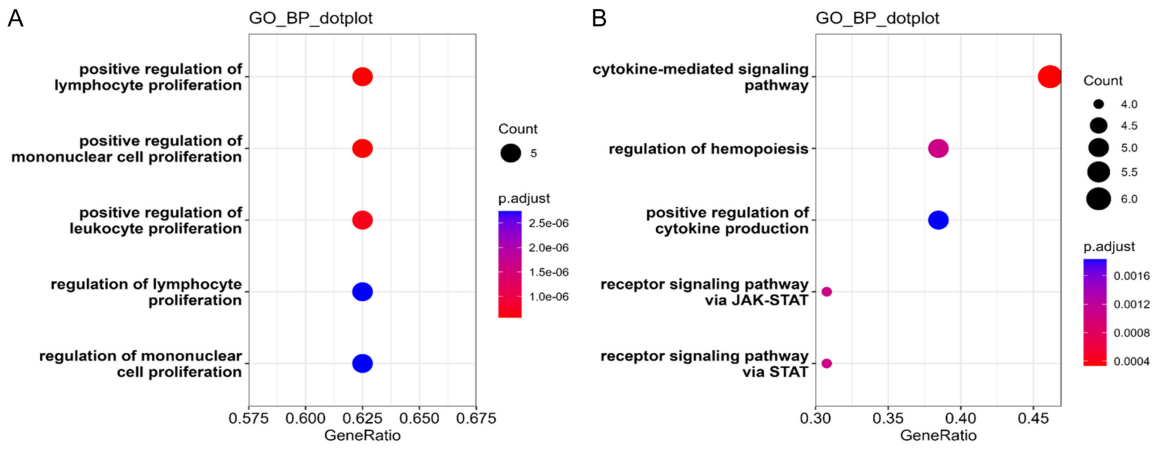

Pathway	Gene	adj.p
Positive regulation of lymphocyte proliferation	NFATC2/MEF2C/HLA-DPA1/IL6ST/CCL19	5.67E-07

Pathway	Gene	adj.p
Positive regulation of cytokine production	CLEC5A/SLC11A1/IL10/IL17A/IFNL1	1.83E-03

Figure 2. Immune pathways associated with long-term survival of metastatic CRC in the discovery dataset. Top 5 pathways revealed by Gene Ontology (GO) enrichment analysis for (A) 8 up-regulated DEGs, and (B) 46 down-regulated DEGs within the tumor microenvironment of long-term survivors, in comparison to short-term survivors. The DEGs involved in the two most significant GO-BP pathways in the tumor microenvironment are illustrated.

Table 3. Univariate Cox regression hazard ratio analysis for three DEGs and the overall survival of metastatic CRC in the discovery dataset

Gene	Hazard ratio (95% CI)	*P* value
SLC11A1	4.09 (1.4-12)	0.012
TNFSF11	3.67 (1.2-11)	0.020
MEF2C	0.34 (0.12-0.94)	0.037

Validation of SLC11A1 as a biomarker for CRC overall survival

The association between SLC11A1, TNFSF11, and overall CRC survival was further examined through the analysis of two TCGA datasets generated using the RNA-seq platform. Patients were sub-grouped into L (i.e., long-term survivors who had overall survival > 50 months) and S (i.e., short-term survivors who had overall survival < 13 months) groups. SLC11A1 substantiated the significant association with CRC survival, which exhibited a hazard ratio (HR) of 2.84 (95% CI (1.5-5.2)) (P=0.00047) in the TCGA dataset 1-L/S (n=93) and an HR of 1.9 (95% CI (1.1-3.2)) (P=0.012) in the TCGA dataset 2-L/S (n=113) (**Table 5**). Conversely, TNFSF11 failed to attain significance in predicting CRC survival within the validation datasets.

Kaplan-Meier survival curve analyses consistently affirmed the substantial associations between SLC11A1 and CRC survival in the TCGA dataset 1-L/S (P=0.00047) and the TCGA dataset 2-L/S (P=0.012) (**Figure 4**). Furthermore, SLC11A1 was significantly associated with the overall survival of all CRC patients in both datasets (P=0.0016 in TCGA dataset 1-all (n=371) and P=0.025 in TCGA dataset 2-all (n=566)) (**Figure 4**).

Receiver operating characteristic (ROC) curve analysis revealed the predictive performance of SLC11A1. In the discovery dataset, SLC11A1 exhibited an AUC of 0.76, a sensitivity of 87%, and a specificity of 60% (**Figure 5**). Additionally, ROC curve analysis within the TCGA dataset 1 showcased SLC11A1 with an AUC of 0.67, a sensitivity of 60%, and a specificity of 73%, while in TCGA dataset 2, SLC11A1 demonstrated an AUC of 0.64, a sensitivity of 59%, and a specificity of 66% (**Figure 5**).

The expression of SLC11A1 in the tumor microenvironment was confirmed through immunohistochemical staining. Specifically, SLC11A1 protein exhibited distinct expression in colorectal cancer tumors, showing elevated levels in cancer cells compared to adjacent normal tissues such as colorectal, lung, or brain tissues (**Figures 6**, **7**). SLC11A1 protein was detected in the cytoplasm, membrane, and nucleus of tumor cells and macrophages within the tissues (**Figure 7**). The expression pattern of

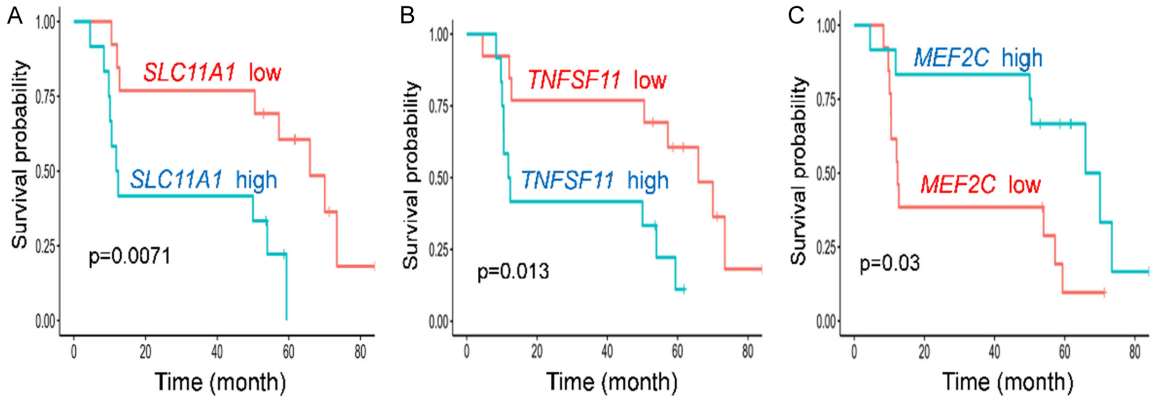

Figure 3. Kaplan-Meier survival analysis for three DEGs in metastatic CRC in the discovery dataset. (A) SLC11A1, (B) TNFSF11, and (C) MEF2C demonstrate statistically significant associations with overall survival in metastatic CRC within the discovery dataset. The median gene expression level was employed as the cutoff value. Survival probabilities for patients with high and low expression of each respective DEG are depicted by the blue and red curves, respectively.

Table 4. Univariate Cox regression hazard ratio analysis for the variables and the overall survival of metastatic CRC in the discovery dataset

Variable	Hazard ratio (95% CI)	*P* value
Age	1.03 (0.99-1.1)	0.10
Histology	1.2 (0.32-4.4)	0.79
Tumor sidedness	2.41 (0.83-7)	0.11
SLC11A1	4.09 (1.4-12)	0.012
TNFSF11	3.67 (1.2-11)	0.02
MEF2C	0.34 (0.12-0.94)	0.22

SLC11A1 protein in tumor tissues mirrored the findings from transcriptome analysis, with lower levels observed in long-term survivors but higher levels in short-term survivors (**Figure 8**).

Discussion

In this study, we comprehensively investigated potential biomarkers within the TME of metastatic CRC patients. Among the various clinical characteristics evaluated, age, histology, tumor sidedness, and the response to targeted therapies exhibited significant associations with CRC survival. Transcriptomic analysis of the TME identified 54 genes that displayed significant differences in expression between long-term and short-term survivors. Particularly noteworthy was the up-regulation of the lymphocyte proliferation pathway observed within the TME of long-term survivors. Conversely, the TME of short-term survivors demonstrated a substantial increase in cytokine production, implying its potential contribution to reduced survival in this patient group. Our univariate COX regression and Kaplan-Meier survival curve analysis uncovered three DEGs (SLC11A1, TNFSF11, and MEF2C) with potential associations with the overall survival of metastatic CRC. Subsequently, SLC11A1 was subjected to rigorous validation through the analysis of two independent TCGA datasets, reaffirming its significance in predicting CRC survival. The ROC analysis further underscored the robust predictive performance of SLC11A1, with an AUC ranging from 0.64 to 0.76, sensitivity between 59% and 87%, and specificity spanning 60% to 73% for predicting CRC survival. The immunohistochemistry analysis validated that SLC11A1 is highly expressed in colorectal cancer cells of short-term survivors and associated with poor prognosis.

SLC11A1 has been reported to encode a late endosomal/lysosomal protein with function as a divalent cation transporter that regulates iron homeostasis in myeloid and macrophages [21]. SLC11A1, also known as natural resistance-associated macrophage protein-1 (NRAMP1), is recruited to the phagosomal membrane after phagocytosis and regulates the host resistance and susceptibility to a range of pathogens [22]. In immune cells, SLC11A1 influences the major histocompatibility complex class II expression and antigen-presenting cell function [23]. It was identified as one of the biomarkers and therapeutic targets for ulcerative colitis [24]. SLC11A1 has been shown to be involved in

Table 5. Univariate Cox regression hazard ratio analysis for SLC11A1 and the overall survival of CRC

Gene	Discovery Dataset (n=25)		TCGA dataset 1-L/S (n=93)		TCGA dataset 2-L/S (n=113)	
	Hazard ratio (95% CI)	*P* value	Hazard ratio (95% CI)	*P* value	Hazard ratio (95% CI)	*P* value
SLC11A1	4.09 (1.4-12)	0.012	2.84 (1.5-5.2)	0.00047	1.9 (1.1-3.2)	0.012

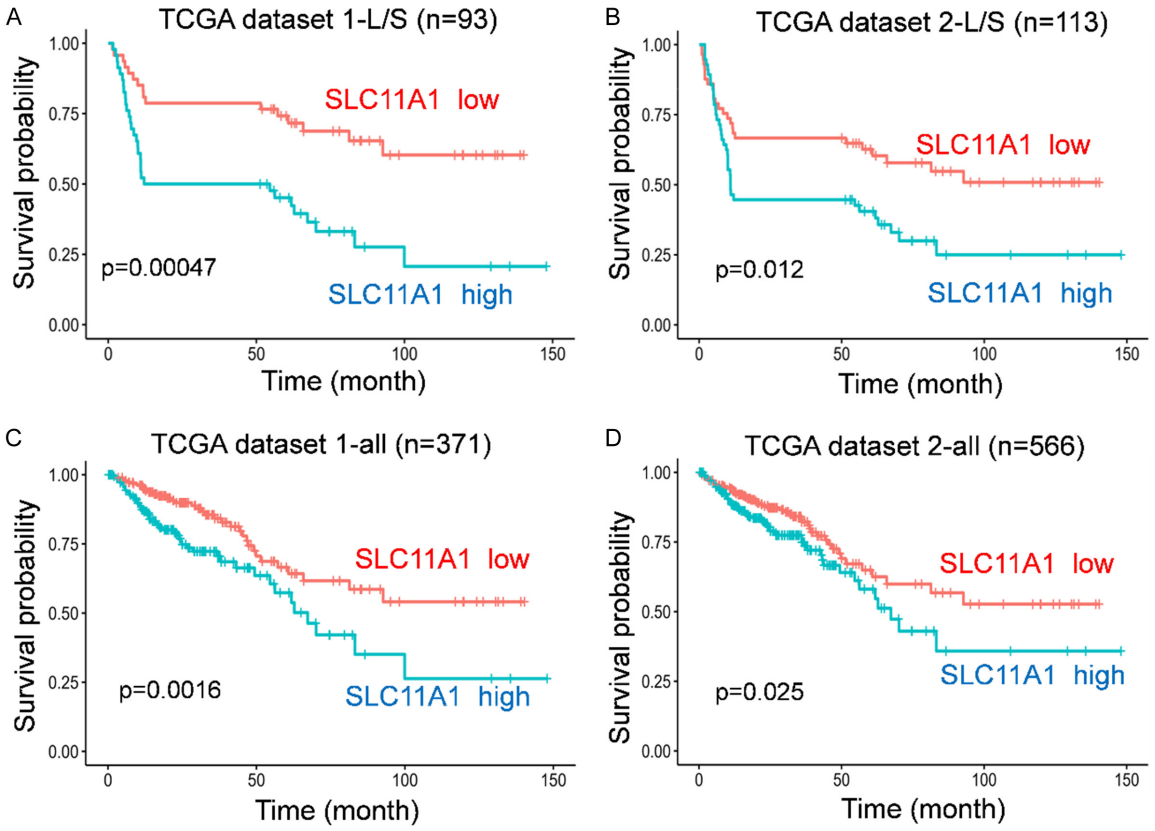

Figure 4. Kaplan-Meier survival analysis of SLC11A1 and overall survival in CRC in the validation datasets. (A) TCGA dataset 1-L/S consisting of 93 patients with defined long/short-term survival duration; (B) TCGA dataset 2-L/S comprising 113 patients with defined long/short-term survival duration; (C) TCGA dataset 1-all encompassing 371 patients; and (D) TCGA dataset 2-all including 566 patients. The median level of gene expression served as the cutoff value. Survival probabilities for patients with high and low expression of the DEG are represented by the blue and red curves, respectively.

innate immunity, infections, inflammation, and autoimmune diseases [25, 26].

Recently, SLC11A1 has been linked to the response and prognosis of different cancers. SLC11A1 was identified as a stratification indicator for immunotherapy or chemotherapy in patients with glioma [27]. The polymorphisms of the SLC11A1 gene are associated with the response to bacillus Calmette-Guerin immunotherapy for superficial bladder cancer, and the risk of prostate cancer [28, 29]. In addition, upregulation of SLC11A1 is associated with poor survival in head and neck cancer patients [30]. SLC11A1 gene was reported to be associated with immune reduction in metastatic melanoma patients treated with targeted therapy [31]. Moreover, SLC11A1 has been suggested to be included in a prognosis signature and used for potential therapeutic drug prediction for renal clear cell carcinoma [32, 33].

SLC11A1 has been linked to the efficacy of immunotherapy in colorectal cancer [34]. Our immunohistochemistry findings are consistent with the quantitative PCR results reported by Ma Y. *et al* [34]. The high expression of SLC11A1 observed in CRC tissues, in contrast to low levels in normal colorectal tissue, supports our conclusion that elevated SLC11A1 expression

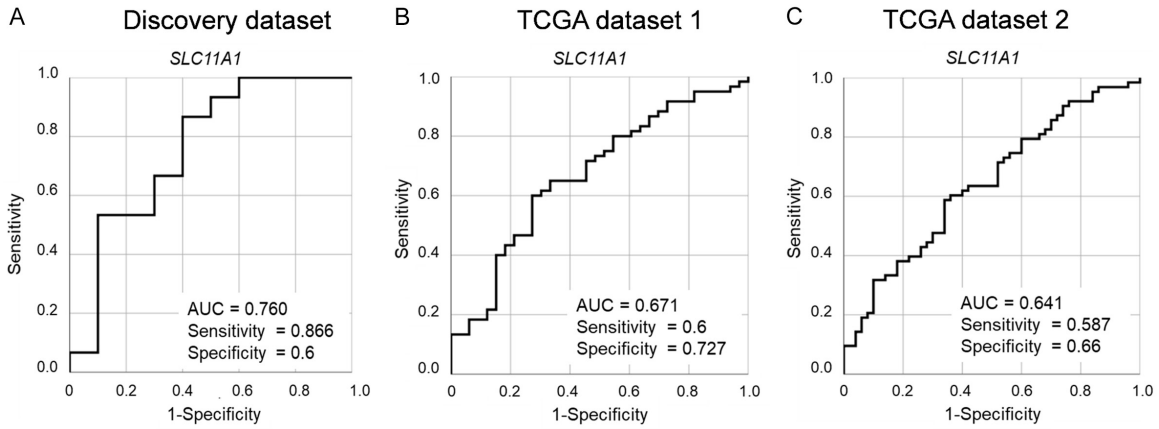

Figure 5. Receiver operating characteristic (ROC) analysis of SLC11A1 for overall survival prediction in CRC. A. In the discovery dataset, the ROC curve for SLC11A1 yields an area under the curve (AUC) of 0.76, demonstrating a sensitivity of 86.6% and a specificity of 60%. B. In TCGA dataset 1, the AUC for SLC11A1 is 0.67, with a sensitivity of 60% and a specificity of 72.7%. C. In TCGA dataset 2, the AUC for SLC11A1 is 0.64, indicating a sensitivity of 59% and a specificity of 66%.

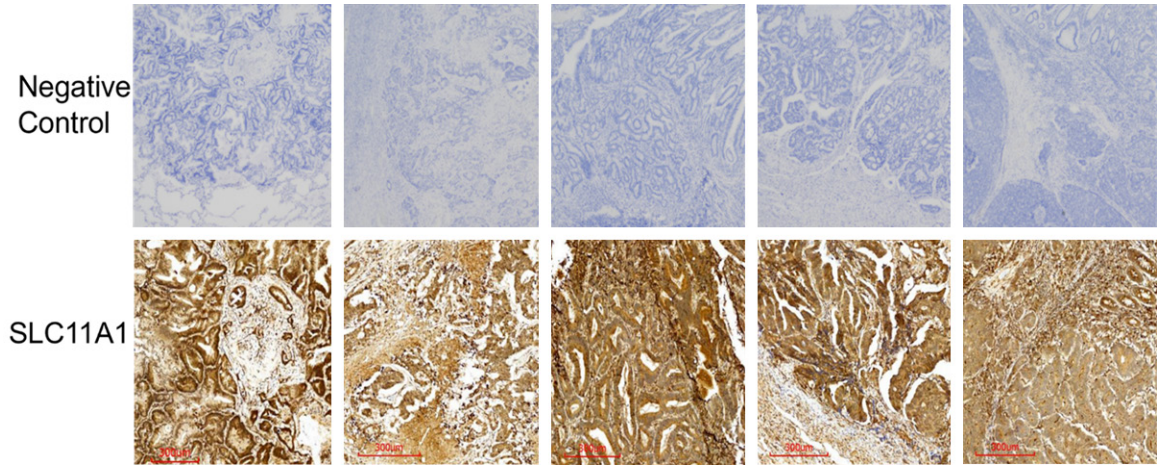

Figure 6. Immunohistochemistry staining of SLC11A1 protein in CRC tumor tissues. Negative controls depict immunohistochemical staining procedures conducted without primary antibody incubation. SLC11A1 expression is observed in the CRC tissue of all patients, with five representative samples displayed.

in the tumor microenvironment correlates with poor prognosis and advanced clinicopathological stages of CRC [34]. Further research is needed to fully understand the specific role of SLC11A1 in the tumor cells and microenvironment of CRC.

In conclusion, our study represents a significant step in identifying potential prognostic biomarkers for CRC survival within the TME. Through a meticulous analysis of 770 immune-related genes in tumor samples, we identified SLC11A1, TNFSF11, and MEF2C significantly associated with the overall survival of metastatic CRC. Of these, SLC11A1 emerged as the most promising candidate, with its association with CRC survival validated in two independent TCGA datasets. The robust performance of SLC11A1 in ROC analysis underscores its potential clinical significance. These results suggest that SLC11A1 could serve as a valuable tool for predicting CRC survival and may find application in enhancing the clinical management of CRC. Further investigations into the mechanistic role of SLC11A1 in the CRC TME are warranted to elucidate its precise contributions and potential therapeutic implications.

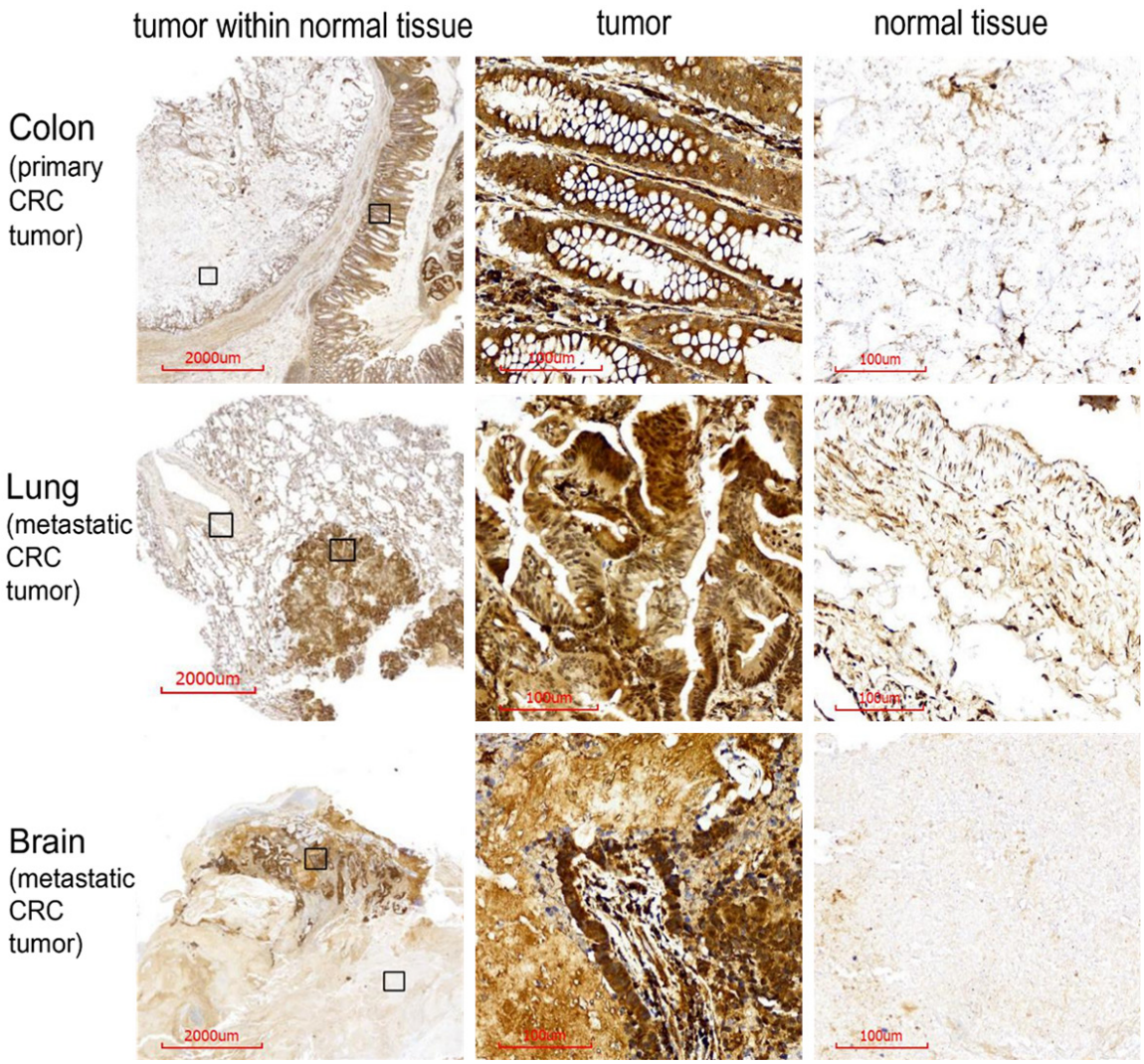

Figure 7. Expression of SLC11A1 protein in colorectal cancer (CRC) tumors in the colon, lung, and brain. Compared to the negative or low expression in adjacent normal tissues, SLC11A1 is prominently detected in CRC tumors and has notable expression in lung macrophages. SLC11A1 protein is observed in the cytoplasm, membrane, and nucleus of tumor cells.

Acknowledgements

We would like to thank the members of the Cancer Vaccine and Immune Cell Therapy core lab at Chang Gung Memorial Hospital for the technical support. This study was supported by the grants of Chang Gung Memorial Hospital (CIRPG3I0041~43 to SIH; CMRPG3K2201~2 to HCH; CIRPG3K0021~2 to HCH), and National Science and Technology Council, Taiwan (MOST 109-2320-B-182A-008-MY3 to SIH; MOST110-2314-B-182A-094 to HCH).

Written informed consent was provided by each participant.

Disclosure of conflict of interest

None.

Abbreviations

AUC, area under the curve; CRC, colorectal cancer; DEG, differentially expressed genes; FFPE, formalin-fixed, paraffin-embedded; GO-BP, Gene Ontology biological pathway; HR, hazard ratio; KRAS, Kirsten rat sarcoma proto-oncogene; MEF2C, myocyte enhancer factor 2C; NFATC2, nuclear factor of activated T cells 2; ROC, receiver operating characteristic; SLC11A1, Solute Carrier Family 11 Member 1;

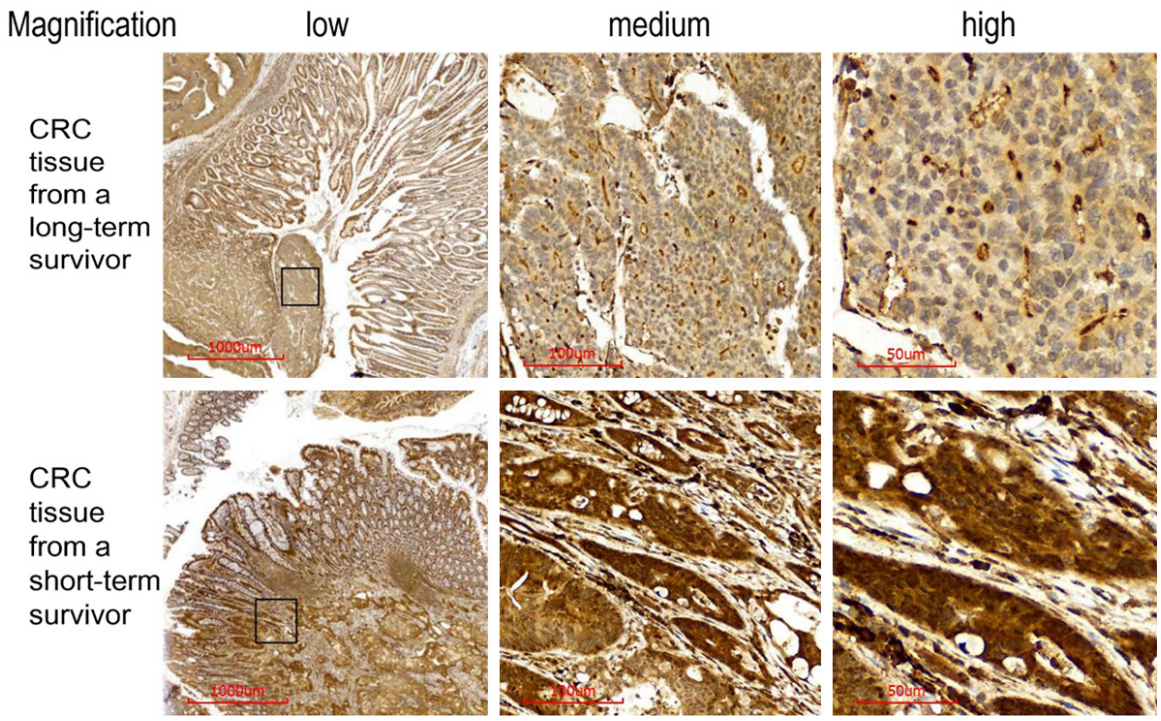

Figure 8. Comparison of SLC11A1 expression in CRC tissues between patients with long- and short-term survival. Representative images show lower levels of SLC11A1 protein in a case of long-term survival compared to higher levels in a case of short-term survival.

TCGA, The Cancer Genome Atlas; TME, tumor microenvironment; TNFSF11, TNF Superfamily Member 11.

Address correspondence to: Dr. Shuen-Iu Hung, Cancer Vaccine and Immune Cell Therapy Core Lab, Chang Gung Immunology Consortium, Department of Medical Research, Chang Gung Memorial Hospital, Linkou Branch, No. 5, Fuxing Street, Guishan District, Taoyuan 333, Taiwan. ORCID: 0000-0001-6531-5538; E-mail: sihung@cgmh.org.tw; sihung@ym.edu.tw; hungshueniu@gmail.com

References

[1] Onyoh EF, Hsu WF, Chang LC, Lee YC, Wu MS and Chiu HM. The rise of colorectal cancer in Asia: epidemiology, screening, and management. Curr Gastroenterol Rep 2019; 21: 36.

[2] Simard J, Kamath S and Kircher S. Survivorship guidance for patients with colorectal cancer. Curr Treat Options Oncol 2019; 20: 38.

[3] Siegel RL, Miller KD, Fedewa SA, Ahnen DJ, Meester RGS, Barzi A and Jemal A. Colorectal cancer statistics, 2017. CA Cancer J Clin 2017; 67: 177-193.

[4] Tricoli JV, Boardman LA, Patidar R, Sindiri S, Jang JS, Walsh WD, McGregor PM 3rd, Camalier CE, Mehaffey MG, Furman WL, Bahrami A, Williams PM, Lih CJ, Conley BA and Khan J. A mutational comparison of adult and adolescent and young adult (AYA) colon cancer. Cancer 2018; 124: 1070-1082.

[5] Sung H, Ferlay J, Siegel RL, Laversanne M, Soerjomataram I, Jemal A and Bray F. Global cancer statistics 2020: GLOBOCAN estimates of incidence and mortality worldwide for 36 cancers in 185 countries. CA Cancer J Clin 2021; 71: 209-249.

[6] Peluso G, Incollingo P, Calogero A, Tammaro V, Rupealta N, Chiacchio G, Sandoval Sotelo ML, Minieri G, Pisani A, Riccio E, Sabbatini M, Bracale UM, Dodaro CA and Carlomagno N. Current tissue molecular markers in colorectal cancer: a literature review. Biomed Res Int 2017; 2017: 2605628.

[7] Kudryavtseva AV, Lipatova AV, Zaretsky AR, Moskalev AA, Fedorova MS, Rasskazova AS, Shibukhova GA, Snezhkina AV, Kaprin AD, Alekseev BY, Dmitriev AA and Krasnov GS. Important molecular genetic markers of colorectal cancer. Oncotarget 2016; 7: 53959-53983.

[8] Cancer Genome Atlas Network. Comprehensive molecular characterization of human colon and rectal cancer. Nature 2012; 487: 330-337.

[9] Zhang B, Wang J, Wang X, Zhu J, Liu Q, Shi Z, Chambers MC, Zimmerman LJ, Shaddox KF, Kim S, Davies SR, Wang S, Wang P, Kinsinger

CR, Rivers RC, Rodriguez H, Townsend RR, Ellis MJ, Carr SA, Tabb DL, Coffey RJ, Slebos RJ and Liebler DC; NCI CPTAC. Proteogenomic characterization of human colon and rectal cancer. Nature 2014; 513: 382-387.

[10] Jin K, Ren C, Liu Y, Lan H and Wang Z. An update on colorectal cancer microenvironment, epigenetic and immunotherapy. Int Immunopharmacol 2020; 89: 107041.

[11] Che Y, Luo Z, Zhang C, Sun N, Gao S and He J. Immune signature of tumor-infiltrating immune cells predicts the prognosis and therapeutic effects in squamous cell carcinoma. Int Immunopharmacol 2020; 87: 106802.

[12] Baba Y, Nomoto D, Okadome K, Ishimoto T, Iwatsuki M, Miyamoto Y, Yoshida N and Baba H. Tumor immune microenvironment and immune checkpoint inhibitors in esophageal squamous cell carcinoma. Cancer Sci 2020; 111: 3132-3141.

[13] Papaioannou NE, Beniata OV, Vitsos P, Tsitsilonis O and Samara P. Harnessing the immune system to improve cancer therapy. Ann Transl Med 2016; 4: 261.

[14] Novoa Díaz MB, Martín MJ and Gentili C. Tumor microenvironment involvement in colorectal cancer progression via Wnt/β-catenin pathway: providing understanding of the complex mechanisms of chemoresistance. World J Gastroenterol 2022; 28: 3027-3046.

[15] Ngambenjawong C, Gustafson HH and Pun SH. Progress in tumor-associated macrophage (TAM)-targeted therapeutics. Adv Drug Deliv Rev 2017; 114: 206-221.

[16] Fridman WH, Miller I, Sautès-Fridman C and Byrne AT. Therapeutic targeting of the colorectal tumor stroma. Gastroenterology 2020; 158: 303-321.

[17] Hoadley KA, Yau C, Hinoue T, Wolf DM, Lazar AJ, Drill E, Shen R, Taylor AM, Cherniack AD, Thorsson V, Akbani R, Bowlby R, Wong CK, Wiznerowicz M, Sanchez-Vega F, Robertson AG, Schneider BG, Lawrence MS, Noushmehr H, Malta TM; Cancer Genome Atlas Network, Stuart JM, Benz CC and Laird PW. Cell-of-origin patterns dominate the molecular classification of 10,000 tumors from 33 types of cancer. Cell 2018; 173: 291-304, e296.

[18] Das K, Chan XB, Epstein D, Te Teh B, Kim KM, Kim ST, Park SH, Kang WK, Rozen S, Lee J and Tan P. NanoString expression profiling identifies candidate biomarkers of RAD001 response in metastatic gastric cancer. ESMO Open 2016; 1: e000009.

[19] Qiu XT, Song YC, Liu J, Wang ZM, Niu X and He J. Identification of an immune-related gene-based signature to predict prognosis of patients with gastric cancer. World J Gastrointest Oncol 2020; 12: 857-876.

[20] Ariyannur PS, Joy RA, Menon V, Paulose RR, Pavithran K and Vasudevan DM. Pilot Nanostring PanCancer pathway analysis of colon adenocarcinoma in a tertiary healthcare centre in Kerala, India. Ecancermedicalscience 2021; 15: 1302.

[21] Blackwell JM, Searle S, Mohamed H and White JK. Divalent cation transport and susceptibility to infectious and autoimmune disease: continuation of the Ity/Lsh/Bcg/Nramp1/Slc11a1 gene story. Immunol Lett 2003; 85: 197-203.

[22] Cunrath O and Bumann D. Host resistance factor SLC11A1 restricts Salmonella growth through magnesium deprivation. Science 2019; 366: 995-999.

[23] Stober CB, Brode S, White JK, Popoff JF and Blackwell JM. Slc11a1, formerly Nramp1, is expressed in dendritic cells and influences major histocompatibility complex class II expression and antigen-presenting cell function. Infect Immun 2007; 75: 5059-5067.

[24] Yarani R, Palasca O, Doncheva NT, Anthon C, Pilecki B, Svane CAS, Mirza AH, Litman T, Holmskov U, Bang-Berthelsen CH, Vilien M, Jensen LJ, Gorodkin J and Pociot F. Cross-species high-resolution transcriptome profiling suggests biomarkers and therapeutic targets for ulcerative colitis. Front Mol Biosci 2023; 9: 1081176.

[25] Awomoyi AA. The human solute carrier family 11 member 1 protein (SLC11A1): linking infections, autoimmunity and cancer? FEMS Immunol Med Microbiol 2007; 49: 324-329.

[26] Dai YD, Marrero IG, Gros P, Zaghouani H, Wicker LS and Sercarz EE. Slc11a1 enhances the autoimmune diabetogenic T-cell response by altering processing and presentation of pancreatic islet antigens. Diabetes 2009; 58: 156-164.

[27] Xu H, Zhang A, Fang C, Zhu Q, Wang W, Liu Y, Zhang Z, Wang X, Yuan L, Xu Y, Shao A and Lou M. SLC11A1 as a stratification indicator for immunotherapy or chemotherapy in patients with glioma. Front Immunol 2022; 13: 980378.

[28] Decobert M, Larue H, Bergeron A, Harel F, Pfister C, Rousseau F, Lacombe L and Fradet Y. Polymorphisms of the human NRAMP1 gene are associated with response to bacillus Calmette-Guerin immunotherapy for superficial bladder cancer. J Urol 2006; 175: 1506-1511.

[29] Manca MA, Scarpa F, Cossu D, Simula ER, Sanna D, Ruberto S, Noli M, Ashraf H, Solinas T, Madonia M, Cusano R and Sechi LA. A multigene-panel study identifies single nucleotide polymorphisms associated with prostate cancer risk. Int J Mol Sci 2023; 24: 7594.

[30] Aleena A, Smiline Girija AS, Balachander K, Vijayashree Priyadharsini J and Arumugam

Paramasivam. Upregulation of SLC11A1 is associated with poor survival in head and neck cancer patients. J RNA Genomics 2021; 17: 1-9.

[31] Berciano-Guerrero MA, Lavado-Valenzuela R, Moya A, delaCruz-Merino L, Toscano F, Valdivia J, Castellón V, Henao-Carrasco F, Sancho P, Onieva-Zafra JL, Navas-Delgado I, Rueda-Dominguez A, Perez-Ruiz E and Alba E. Genes involved in immune reinduction may constitute biomarkers of response for metastatic melanoma patients treated with targeted therapy. Biomedicines 2022; 10: 284.

[32] Li W, Meng X, Yuan H, Xiao W and Zhang X. A novel immune-related ceRNA network and relative potential therapeutic drug prediction in ccRCC. Front Genet 2022; 12: 755706.

[33] Yao ZY, Xing C, Liu YW and Xing XL. Identification of two immune related genes correlated with aberrant methylations as prognosis signatures for renal clear cell carcinoma. Front Genet 2021; 12: 750997.

[34] Ma Y, Zhan L, Yang J and Zhang J. SLC11A1 associated with tumor microenvironment is a potential biomarker of prognosis and immunotherapy efficacy for colorectal cancer. Front Pharmacol 2022; 13: 984555.